REPORT DOCUMENTATION PAGE

Form Approved
OMB No. 0704-01-0188

PLEASE DO NOT RETURN YOUR FORM TO THE ABOVE ADDRESS.

1. REPORT DATE *(DD-MM-YYYY)*	2. REPORT TYPE	3. DATES COVERED *(From - To)*
25-08-2005	REPRINT	

4. TITLE AND SUBTITLE

Rotational and spin-orbit distribution of NO observed by MIPAS/ENVISAT during the solar storm of October/November 2003

5a. CONTRACT NUMBER

5b. GRANT NUMBER

5c. PROGRAM ELEMENT NUMBER
61102F

6. AUTHORS

J.L. Gardner*, M. Lopez-Puertas**, B. Funke**, S.M. Miller, S. J. Lipson, and R.D.Sharma

5d. PROJECT NUMBER
2303

5e. TASK NUMBER
HS

5f. WORK UNIT NUMBER
A1

7. PERFORMING ORGANIZATION NAME(S) AND ADDRESS(ES)

Air Force Research Laboratory /VSBYH
29 Randolph Road
Hanscom AFB, MA 01731-3010

8. PERFORMING ORGANIZATION REPORT NUMBER
AFRL-VS-HA-TR-2005-1198

9. SPONSORING/MONITORING AGENCY NAME(S) AND ADDRESS(ES)

10. SPONSOR/MONITOR'S ACRONYM(S)
AFRL/VSBYH

11. SPONSOR/MONITOR'S REPORT NUMBER(S)

12. DISTRIBUTION/AVAILABILITY STATEMENT

Approved for public release; distribution unlimited.

13. SUPPLEMENTARY NOTES

REPRINTED FROM: Journal of Geophysical Research, Vol. 110, A09S34 doi:10.1029/2004JA010937, 2005, © 2005, American Geophysical Union. *Stewart Radiance Laboratory, Bedford, MA 01730. **Instituto de Astrofisico de Andalucia (CSIC), Granada, Spain.

14. ABSTRACT

Aurorally enhanced 5.3 μm emission from nitric oxide was observed by the MIPAS instrument on board the ENVISAT satellite during the solar storm of October/November 2003. Spectral modeling of the NO($\Delta v = 1$) fundamental band emissions was performed in order to determine the NO rotational and spin-orbit distributions. In the thermosphere, NO($\Delta v = 1$) is produced by collisional excitation of NO($v = 0$) by O atoms and also by the chemical reactions of N(^{4}S) and N(^{2}D) atoms, resulting in enhanced chemical formation of NO. In the MIPAS data taken during the solar storm, strong NO signal levels and increased rotational temperatures indicated high levels of auroral activity. A comparison of the data from October/November 2003 with data taken during a quiescent period in June 2003 showed that NO($v = 1$) produced by N + O_2 has a hotter spin-orbit distribution than NO($v = 1$) produced by O atom collisional excitation. The results imply that the spin-orbit ratio may be useful for identifying different sources of NO in the thermosphere. In addition, the NO($v = 1$) spin-orbit distributions were found not to be in local thermodynamic equilibrium (non-LTE) for both quiescent and auroral conditions. The non-LTE effects must be taken into account in order to accurately retrieve atmospheric NO concentrations from 5.3 μm emissions.

15. SUBJECT TERMS

Nitric oxide
Aurora
Spin-orbit
Rotational temperature
Thermodynamic equilibrium
Infrared spectroscopy
Vibrational excitation

16. SECURITY CLASSIFICATION OF:			17. LIMITATION OF ABSTRACT	18. NUMBER OF PAGES	19a. NAME OF RESPONSIBLE PERSON
a. REPORT	b. ABSTRACT	c. THIS PAGE			Steven Lipson
UNCL	UNCL	UNCL	UNL		19B. TELEPHONE NUMBER *(Include area code)* (781) 377-3626

JOURNAL OF GEOPHYSICAL RESEARCH, VOL. 110, A09S34, doi:10.1029/2004JA010937, 2005

Rotational and spin-orbit distributions of NO observed by MIPAS/ ENVISAT during the solar storm of October/November 2003

J. L. Gardner,[1] M. Lopéz-Puertas,[2] B. Funke,[2] S. M. Miller,[3] S. J. Lipson,[3] and R. D. Sharma[3]

Received 30 November 2004; revised 6 April 2005; accepted 29 April 2005; published 25 August 2005.

[1] Aurorally enhanced 5.3 μm emission from nitric oxide was observed by the MIPAS instrument on board the ENVISAT satellite during the solar storm of October/November 2003. Spectral modeling of the NO($\Delta v = 1$) fundamental band emissions was performed in order to determine the NO rotational and spin-orbit distributions. In the thermosphere, NO($v = 1$) is produced by collisional excitation of NO($v = 0$) by O atoms and also by the chemical reactions of N(^{4}S) and N(^{2}D) atoms with O_2. There are no measurements of the nascent spin-orbit distribution of NO produced by the reaction of N atoms with O_2. Auroral activity leads to increased production of N(^{4}S) and N(^{2}D) atoms, resulting in enhanced chemical formation of NO. In the MIPAS data taken during the solar storm, strong NO signal levels and increased rotational temperatures indicated high levels of auroral activity. A comparison of the data from October/November 2003 with data taken during a quiescent period in June 2003 showed that NO($v = 1$) produced by N + O_2 has a hotter spin-orbit distribution than NO($v = 1$) produced by O atom collisional excitation. The results imply that the spin-orbit ratio may be useful for identifying different sources of NO in the thermosphere. In addition, the NO($v = 1$) spin-orbit distributions were found not to be in local thermodynamic equilibrium (non-LTE) for both quiescent and auroral conditions. The non-LTE effects must be taken into account in order to accurately retrieve atmospheric NO concentrations from 5.3 μm emissions.

Citation: Gardner, J. L., M. Lopéz-Puertas, B. Funke, S. M. Miller, S. J. Lipson, and R. D. Sharma (2005), Rotational and spin-orbit distributions of NO observed by MIPAS/ENVISAT during the solar storm of October/November 2003, *J. Geophys. Res.*, *110*, A09S34, doi:10.1029/2004JA010937.

1. Introduction

[2] From 19 October to 4 November 2003, strong solar storms were produced by a large number of energetic solar flares and coronal mass ejections. Over the 2-week period, 12 X-class solar flares erupted, and the X-17 class flare on 28 October created one of the largest geomagnetic storms on record [*Simpson*, 2003]. Solar wind speeds exceeding 1850 km/s were measured on 29 October due to the shock produced by the X-17 class flare [*Skoug et al.*, 2004]. Previous studies have observed significant enhancements in nitric oxide density following auroral events [e.g., *Siskind et al.*, 1998; *Solomon et al.*, 1999]. Recently, *Mlynczak et al.* [2003] measured a factor of 5 to 7 increase in the 5.3 μm limb radiance during the solar storm of April 2002 using the SABER (Sounding of the Atmosphere using Broadband Emission Radiometry) instrument on board NASA's TIMED (Thermosphere-Ionosphere-Mesosphere Energetics and Dynamics) satellite.

[3] During the solar storm of October/November 2003, the MIPAS instrument on board the ENVISAT satellite measured enhanced NO 5.3 μm emissions. The European Space Agency (ESA) launched ENVISAT (Earth observing Environmental Satellite), an advanced polar-orbiting satellite at an altitude of ~800 km, in March 2002. The MIPAS (Michelson Interferometer for Passive Atmospheric Sounding) instrument is a Fourier transform spectrometer that measures earthlimb emissions in the 4.15–14.6 μm (685–2410 cm^{-1}) range with unapodized resolution of 0.035 cm^{-1} [*European Space Agency (ESA)*, 2000]. The data have the highest spectral resolution ever recorded in the upper atmosphere over such a wide spectral range. The spectral resolution of the instrument permits detailed study of the rotational and spin-orbit state distributions of NO(Ω = 1/2, 3/2) in the upper atmosphere.

[4] In this paper, MIPAS data taken under both auroral and quiescent conditions are analyzed and compared with the results of a previous study by *Lipson et al.* [1994]. The earlier study was based on measurements of NO 5.3 μm emission made by the CIRRIS 1A (Cryogenic Infrared Radiance Instrumentation for Shuttle) experiment. The

[1]Stewart Radiance Laboratory, Bedford, Massachusetts, USA.
[2]Instituto de Astrofísica de Andalucía (CSIC), Granada, Spain.
[3]Space Vehicles Directorate, Air Force Research Laboratory, Hanscom Air Force Base, Massachusetts, USA.

0148-0227/05/2004JA010937$09.00

1 cm^{-1} resolution of the instrument was only sufficient to partially resolve the NO spin-orbit splitting. Lipson et al. determined that NO spin-orbit distributions are not in LTE in the thermosphere under quiescent conditions. Previous investigations of NO concentrations in the upper atmosphere have relied on the assumption that the rotational and spin-orbit populations are in LTE [*Clancy et al.*, 1992; *Ballard et al.*, 1993]. Lipson et al. demonstrated that this assumption could lead to significant errors in the determination of NO density. A number of studies have highlighted the importance of including non-LTE vibrational, rotational, and spin state effects in models of NO 5.3 μm emission [e.g., *Kaye and Kumer*, 1987; *Funke et al.*, 2000; *Funke et al.*, 2001]. Recently, *Funke and López-Puertas* [2000] developed a comprehensive non-LTE model of NO state distributions for altitudes from the ground to 200 km for quiescent atmospheric conditions. Using the model, *Funke et al.* [2001] demonstrated that ignoring non-LTE effects will lead to considerable errors in modeled 5.3 μm radiances (up to 20% at the line center positions) and create instabilities and inaccuracies (~20%) in the retrieval of stratospheric NO. Non-LTE processes in the thermosphere influence stratospheric NO retrievals because thermospheric emissions contribute significantly to observations at stratospheric tangent heights.

[5] Being able to identify and quantify the contributions of different sources of NO(v) is important for understanding the energy budget of the upper atmosphere. There are three mechanisms that produce vibrationally excited NO and lead to 5.3 μm emission in the terrestrial thermosphere. The first mechanism, which is responsible for the majority of 5.3 μm emission in the thermosphere, is the vibrational excitation of NO($v = 0$) by impacts with atomic oxygen:

$$\text{(R1)} \qquad NO(v = 0) + O \rightarrow NO(v = 1) + O.$$

NO($v = 1$) produced by process (1) has a Boltzmann rotational distribution that is subthermal [*Sharma et al.*, 1996a; *Sharma and Duff*, 1997]. The nascent NO($v = 1$) rotational temperature is approximately 25% lower than the translational temperature of the atmosphere above 130 km. At lower altitudes, the rotational temperature is thermalized to the translational temperature of the atmosphere by collisions before the molecule emits a photon. At higher altitudes, the NO($v = 1$) radiative rate ($A_v = 13\ s^{-1}$) becomes more dominant than the collisional rate, keeping the NO($v = 1$) rotational state distributions in non-LTE. Collisional excitation of NO by O atoms is the most important atmospheric cooling process in the 110–300 km altitude range because it converts kinetic energy to radiative energy which is released to space.

[6] The inelastic collision process (1) has a rate coefficient of $2.8 \times 10^{-11}\exp(-2700/T)$ $cm^3\ s^{-1}$ based on theoretical calculations [*Duff and Sharma*, 1997]. A more recent experimental measurement of the rate constant reports a higher preexponential factor of 4.2×10^{-11} [*Hwang et al.*, 2003]. Although the NO($v = 0$) density peaks around 105 km altitude, the 5.3 μm emission from process (1) actually peaks near 130 km altitude because of the $\exp(-2700/T)$ factor in the rate coefficient [*Armstrong et al.*, 1994; *Sharma et al.*, 1996a]. The excitation of NO($v = 0$) by inelastic collisions with O_2 and N_2 is slow compared with the rate of energy transfer with O atoms. The room temperature rate coefficients for the production of NO($v = 1$) by impacts with O_2 and N_2 are about 3 and 5 orders of magnitude smaller than that for process (1) [*Murphy et al.*, 1975]. Since the densities of O_2 and N_2 above 100 km altitude are not high enough to compensate for the lower rate coefficients, inelastic collisions with O atoms are the only significant source of NO collisional vibrational excitation in the thermosphere.

[7] Collisional excitation of NO by O atoms can also produce NO in higher-energy vibrational states. The calculated rate coefficient of the process

$$\text{(R2)} \qquad NO(v = 0) + O \rightarrow NO(v = 2) + O$$

is $1.4 \times 10^{-11}\exp(-5400/T)$ cm^3s^{-1} [*Duff and Sharma*, 1997]. For the temperatures normally encountered at about 130 km altitude ($T \sim 600$ K), the $2 \rightarrow 1$ vibrational band emission near 5.3 μm due to process (2) is about 1% of the $1 \rightarrow 0$ vibrational band emission due to process (1). The calculated rate coefficient of the process

$$\text{(R3)} \qquad NO(v = 1) + O \rightarrow NO(v = 2) + O$$

is $1.4 \times 10^{-11}\exp(-2700/T)$ $cm^3\ s^{-1}$ [*Duff and Sharma*, 1997]. At midlatitudes the fraction of NO molecules in the $v = 1$ vibrational level at 130 km altitude around local noon is about 0.4%. Under these conditions the $2 \rightarrow 1$ vibrational band emission near 5.3 μm due to process (3) is about 0.2% of the $1 \rightarrow 0$ vibrational band emission due to process (1). Overall, more than 98% of the 5.3 μm emission resulting from the impacts of NO with O is due to reaction (1).

[8] The second mechanism leading to 5.3 μm emission in the thermosphere is the production of highly rotationally and vibrationally excited NO by the reaction

$$\text{(R4)} \qquad N(^4S) + O_2 \rightarrow NO(v, j) + O.$$

Although this reaction is exothermic by 1.385 eV, the entrance channel has an energy barrier of 0.3 eV. Therefore only those atom-molecule pairs which have relative translational energy greater than 0.3 eV are able to react. A substantial fraction of the exothermicity of this reaction goes toward producing highly rotationally excited NO [*Duff et al.*, 1994]. In the CIRRIS 1A data, R-branch bandheads at high j were observed mainly from the $1 \rightarrow 0$ and $2 \rightarrow 1$ bands of NO under quiescent daytime and nighttime conditions. *Sharma et al.* [1993, 1996b, 1998] have determined that the rotational bandheads were the result of emissions from nascent NO produced by reaction (4). *Sharma et al.* [1998] have also shown that the NO bandheads observed at lower tangent altitudes (<130 km) have their origin in the hotter, higher altitudes where some of the thermalized $N(^4S)$ and O_2 pairs have enough energy to overcome the 0.3 eV barrier to the reaction.

[9] The third mechanism leading to 5.3 μm emission in the thermosphere is the production of highly rotationally and vibrationally excited NO by the reaction

$$(R5) \qquad N(^2D) + O_2 \rightarrow NO(v, j) + O.$$

This reaction is more important during the quiescent daytime than at nighttime because the concentration of $N(^2D)$ atoms is negligible during the night [*Rusch et al.*, 1991]. The reaction has an exothermicity of 3.76 eV and produces NO in high rotational states and vibrational levels up to $v = 14$ [*Duff et al.*, 2003; *Miller et al.*, 2003]. The 5.3 μm chemiluminescence due to this reaction is therefore spread over hundreds of transitions. For this reason, the quiescent daytime emission from nascent NO produced by reaction (5) was below the signal threshold of the CIRRIS 1A data and was not observed. Auroral activity leads to enhanced production of both $N(^4S)$ and $N(^2D)$ atoms in the upper atmosphere [*Vitt et al.*, 2000]. Under strong auroral dosing, emission from reaction (5) was observed by MSX (Midcourse Space Experiment) and CIRRIS 1A and has been modeled by *Sharma et al.* [2001], *Dothe et al.* [2002], and *Duff et al.* [2005]. The nascent spin-orbit distributions of NO produced by reactions (4) and (5) have never been measured. The high spectral resolution MIPAS data analyzed in this paper, taken under both quiescent and highly perturbed auroral conditions, provide important new information about the $NO(v = 1)$ state distributions.

2. Data Acquisition and Processing

[10] Emissions of 5.3 μm were recorded by the MIPAS instrument [*ESA*, 2000] on board the ENVISAT satellite during the solar storm of October/November 2003. Under normal operating conditions, MIPAS starts the earthlimb scans at 68 km tangent altitude and descends to 8 km tangent altitude. For each height step a single interferometer sweep is performed and interferograms are recorded in five spectral bands using Hg:Cd:Te detectors. The instrument records emissions in the 685–2410 cm^{-1} range and has an unapodized resolution of 0.035 cm^{-1}. The sensitivity of the instrument is 50 nW/(cm^2 sr cm^{-1}) on the long wavelength side and 4.2 nW/(cm^2 sr cm^{-1}) on the short wavelength side. The data reported in this paper were recorded by detector D which covers a spectral range of 1820–2410 cm^{-1}. Typically, 16 tangent heights are sampled per scan, and a total of 75 complete elevation scans are performed during an orbit lasting 100 minutes. On 14 June 2003, the MIPAS instrument was operated in a special mode that sampled thermospheric tangent heights.

[11] The MIPAS spectra were fit with a nonlinear, iterative least-squares technique used in previous studies [*Armstrong et al.*, 1994; *Lipson et al.*, 1994]. The NO line positions were derived from the spectroscopic parameters of *Amiot* [1982]. The rotation-vibration line strengths were calculated using Hönl-London formulae [*Kovacs*, 1969] along with the band-averaged Einstein coefficients from *Rawlins et al.* [1998]. Spectral fitting of the 5.3 μm emission was used to determine the NO vibrational, rotational, and spin-orbit distributions during both auroral and quiescent atmospheric conditions. The auroral spectra were taken at a tangent altitude of ~68 km, the highest tangent altitude recorded during the October/November 2003 solar storm. The quiescent data from June 2003 were taken at tangent altitudes ranging from 68 to 164 km.

3. Results and Discussion

3.1. Origin of Observed 5.3 μm Emission

[12] In order to analyze the MIPAS data, it is necessary to consider which altitudes are contributing to the NO signal. It is important to take into account both the line of sight (LOS) path through the atmosphere and the variability of $NO(v = 1)$ production as a function of altitude. Interpretation of the MIPAS data taken during the solar storm of October/November 2003 is complicated by the fact that the LOS at a tangent altitude (H_0) of 68 km includes contributions from radiation originating at higher altitudes. The length of the LOS between altitudes $H_0 + n + 1$ and $H_0 + n$ is

$$(R6) \qquad L_{H_0+n+1,H_0+n} = 2(12920 + 2H_0)^{\frac{1}{2}}\left(\sqrt{(n+1)} - \sqrt{n}\right).$$

Thus the length of the LOS decreases rapidly at altitudes greater than the tangent altitude. However, most of the 5.3 μm emission observed by MIPAS at a tangent altitude of 68 km is likely produced in the thermosphere due to the altitude dependence of the $NO(v)$ formation mechanisms. For example, $NO(v = 1)$ radiance produced by O atom collisional excitation peaks near an altitude of 130 km. The production of $NO(v)$ from the $N(^4S) + O_2$ reaction is most important at altitudes above 150 km, where the $N(^4S)$ atoms have sufficient kinetic energy to overcome the reaction energy barrier. Production of $NO(v)$ due to the $N(^2D) + O_2$ reaction is greatest above 100 km [*Sharma et al.*, 1998; *Funke and López-Puertas*, 2000]. Under auroral conditions, increased production of $N(^4S)$ and $N(^2D)$ atoms over a variety of altitudes results in the enhanced production of $NO(v)$ by chemical reactions. Measurements made during an auroral event in May 1998 showed that NO density and electron energy deposition both peaked at an altitude of 106 km [*Sætre et al.*, 2004]. Auroral models indicate that in the lower thermosphere the $N(^2D) + O_2$ reaction is the most important source of chemically produced $NO(v)$ [*Sharma et al.*, 2001; *Dothe et al.*, 2002].

[13] In the mesosphere, the dominant mechanism for 5.3 μm radiative emission is the absorption of solar and upwelling tropospheric radiation, $NO(v = 0) + h\nu \rightarrow NO(v = 1)$, by ambient NO [*Sharma et al.*, 1998; *Funke and López-Puertas*, 2000]. Radiative excitation does not change the NO rotational and spin state distributions due to the rotational selection rules ($\Delta j = 0, \pm 1$) and the spin selection rule ($\Delta\Omega = 0$). Therefore the emitted radiation has the local $NO(v = 0)$ rotational temperature and spin state distribution. Overall, very little mesospheric NO emission is expected to be observed by MIPAS based on atmospheric modeling simulations [*Funke et al.*, 2001]. In the stratosphere, the two mechanisms that produce 5.3 μm emission are the photodissociation of NO_2 leading to $NO(v, j) + O$ and the reaction $NO_2 + O \rightarrow NO(v, j) + O_2$ [*Kaye and Kumer*, 1987; *Funke and López-Puertas*, 2000]. These emissions do not directly contribute to the signal because they originate from altitudes below the 68 km tangent

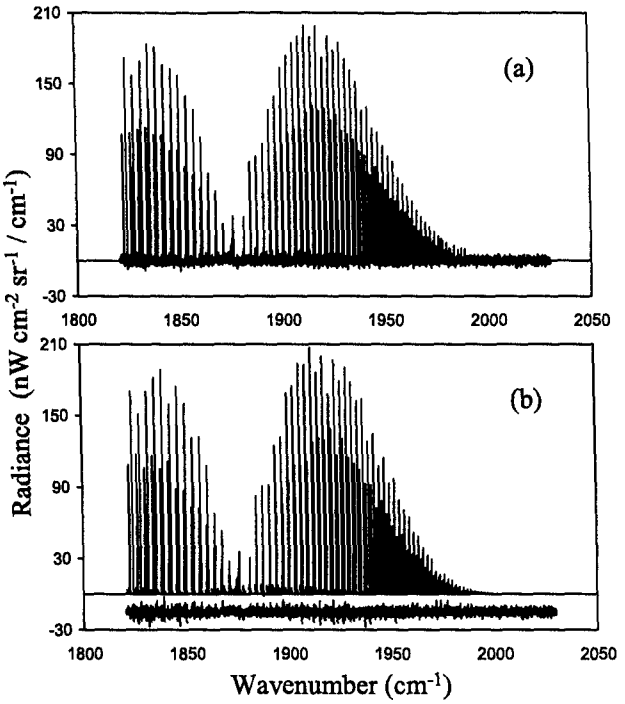

Figure 1. (a) MIPAS NO 5.3 μm emission spectrum recorded on 29 October 2003 under auroral conditions at a latitude of −54° and a tangent altitude of 68 km. (b) Least-squares fit to spectrum (a) with a rotational temperature of 803 K and a spin-orbit Ω = 1/2 fraction of 0.616. The residuals are shown below the spectrum.

altitude of the MIPAS data. Although it is possible that upwelling radiation from the stratosphere could be resonantly scattered into the LOS at higher altitudes, the small densities of NO(v = 1) in the stratosphere make this resonant scattering very unlikely. Having excluded other possible emission sources, we conclude that the NO 5.3 μm radiation observed by the MIPAS instrument at a tangent altitude of 68 km originates almost entirely from the thermosphere.

3.2. Spectral Analysis of 5.3 μm NO Emission

[14] A MIPAS spectrum recorded on 29 October during a period of intense geomagnetic activity is presented in Figure 1a. The spectrum was taken during daytime at a latitude of −54° and a tangent altitude of 68 km. The two NO spin-orbit populations are readily observed in the spectrum, with the more intense lines originating in the Ω = 1/2 manifold. Spectral modeling of the MIPAS data has been conducted in order to determine the NO rotational and spin-orbit distributions in the observed 5.3 μm emissions. Figure 1b is a least-squares fit to the spectrum in Figure 1a assuming a Boltzmann rotational distribution and allowing the model spin-orbit ratio to vary. The small residuals, shown at the bottom of Figure 1b, demonstrate that the data is well fit by the model for a rotational temperature of 803 K and a spin-orbit ratio (Ω = 1/2 fraction of the total spin-orbit population) of 0.616, which corresponds to a spin temperature of 365 K. If the spin-orbit populations were in equilibrium with the rotational temperature, a spin-orbit ratio of 0.55 would be predicted. Instead, the spin-orbit temperature is more than 400 K colder than the rotational temperature. The spin-orbit ratio (Ω = 3/2: Ω = 1/2) is related to temperature by the expression exp(−$\Delta E/kT$) with a spin-orbit ΔE separation of ~120 cm^{-1} for NO. The Ω = 1/2 fraction of the total spin-orbit population can easily be calculated by the equation 1/(1 + (Ω = 3/2: Ω = 1/2)). Under quiescent conditions, *Lipson et al.* [1994] also observed subthermal NO spin-orbit populations. The strong signal levels and the high rotational temperature of the spectrum in Figure 1 indicate that the data were taken under auroral conditions.

[15] In Figure 2, a small section of the data from Figure 1 has been plotted in order to show the spectral detail. The figure illustrates the excellent resolution of the MIPAS instrument and shows that the spectral resolution is more than sufficient to fully resolve the NO spin-orbit splitting. When analyzing the MIPAS data, the model tries to fit both the NO(v = 1) and NO(v = 2) populations. Emission from NO(v = 2) is close to the detection threshold of the instrument and can only be observed in the data sets with the highest signal levels. The model fit to the NO(v = 2) emission is shown in Figure 2 below the data. Owing to the low signal levels, it is difficult to accurately determine the rotational temperature or the spin-orbit ratio from the 2 → 1 emission. In Figure 2, the NO(v = 2) signal is approximately 3% of the emission from the NO(v = 1) state. Emission from NO(v = 2), produced by collisional excitation of NO by O atoms, is expected to be less than 2% of the total 5.3 μm emission. The additional observed 2 → 1 emission may be due to NO(v = 2) produced by the chemical reactions of N(^{2}D) and N(^{4}S) atoms with O_2. However, it is important to note that there are no R-branch high j bandheads visible in the data from Figure 1. In the CIRRIS 1A experiment, bandheads from highly rotationally excited NO (T_{Rot} ~ 5000 K) were observed under auroral and quiescent conditions [*Armstrong et al.*, 1994; *Sharma et al.*, 1998; *Dothe*

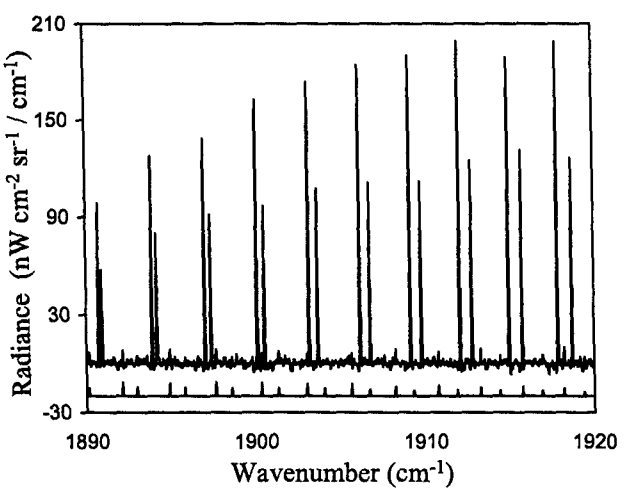

Figure 2. A section of data from Figure 1 showing the high spectral resolution of the MIPAS instrument. The two NO spin-orbit populations are clearly resolved with the more intense lines originating in the Ω = 1/2 spin state. The model fit to the NO(v = 2) emission is shown below the spectrum. The NO(v = 2) signal is approximately 3% of the NO(v = 1) signal.

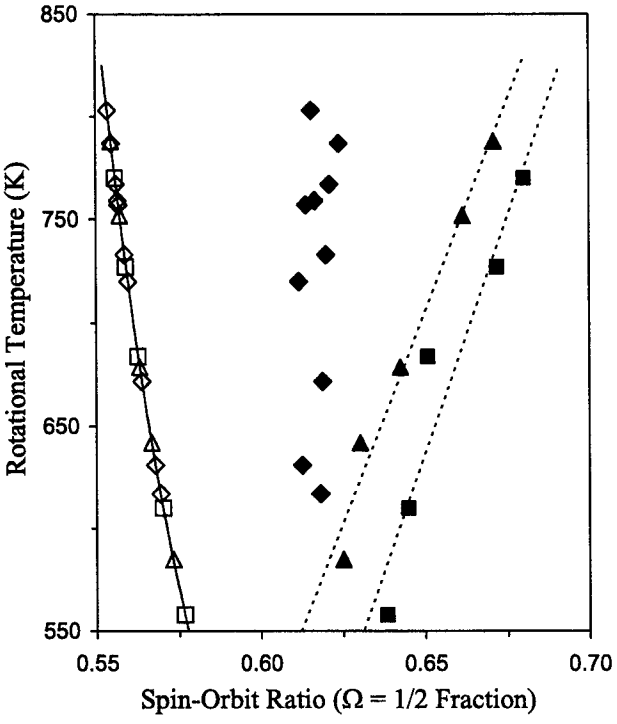

Figure 3. Comparison of data from the solar storm with quiescent data taken in June 2003. Diamonds represent auroral day/night/twilight data at 68 km tangent altitude. Triangles represent daytime quiescent data. Squares represent nighttime quiescent data. Each quiescent data point was taken at a different tangent altitude ranging from ~120 to 160 km in 10 km steps. The dashed lines are simple linear fits to the quiescent data. The open symbols are the predicted spin-orbit $\Omega = 1/2$ fractions assuming equilibrium conditions.

et al., 2002]. The $1 \rightarrow 0$ and $2 \rightarrow 1$ rotationally excited bandheads, located at 2021 and 1990 cm^{-1}, respectively, are produced by the reactions of $N(^2D)$ and $N(^4S)$ atoms with O_2. The bandheads were not observed by MIPAS during the solar storm because the higher temperature of the MIPAS instrument and detector, compared with the CIRRIS 1A instrument, produces noise levels greater than the signal level of the NO bandheads.

[16] A comparison of data from October/November 2003 with data taken during a quiescent period in June 2003 is presented in Figure 3 in order to investigate the effects of auroral activity on the NO rotational and spin state distributions. Figure 3 is a plot of NO rotational temperature versus NO spin-orbit ratio ($\Omega = 1/2$ fraction of the total spin-orbit population). The filled symbols are the results of spectral modeling of the MIPAS 5.3 μm emission from NO(v = 1). The data points with diamond symbols were recorded during auroral conditions on 29 October at a tangent altitude of 68 km. Of the auroral data points, four were taken during the daytime, four were taken at nighttime, and two were taken at twilight for latitudes ranging from −48° to −82°. A summary of the conditions and results for the auroral NO data points is presented in Table 1. The data points with triangle symbols were recorded during quiescent daytime conditions on 14 June at a latitude of 75°. The data points with square symbols were recorded during quiescent nighttime conditions on 14 June at a latitude of −58°. Each data point for the quiescent data was taken at a different tangent altitude ranging from ~120 to 160 km in 10 km steps. A summary of the conditions and results for the quiescent NO data points is presented in Table 2. Under quiescent conditions, the NO rotational temperature above 130 km roughly scales with tangent altitude and is about 25% lower than the translational temperature of the atmosphere [*Lipson et al.*, 1994; *Sharma and Duff*, 1997]. In Figure 3, the dashed lines are simple linear fits to the quiescent daytime data (left) and nighttime data (right). The main source of error in the determination of the NO spin-orbit ratios is the background noise in the spectra. Because the spin-orbit ratio is calculated based on the relative strengths of the $\Omega = 1/2$ and 3/2 components, the results do not depend on the absolute calibration of the MIPAS instrument. The estimated error in the spin-orbit ratios of the auroral data points in Figure 3 is less than 1% due to the strong signal levels. The estimated error in the spin-orbit ratios of the quiescent data points ranges from ~1% at the lowest tangent altitudes to ~3% at the highest tangent altitude due to decreasing signal levels as a function of altitude above 130 km.

[17] The open symbols in Figure 3 are the $\Omega = 1/2$ fractions that would be predicted for each data point if the NO spin-orbit populations were in equilibrium with the rotational temperature. As shown in Figure 3, the NO $\Omega = 1/2$ fraction is expected to decrease with increasing temperature under equilibrium conditions. In contrast, all of the MIPAS data points have subthermal NO spin-orbit populations, and for quiescent conditions, the $\Omega = 1/2$ fractions increase with increasing temperature. *Lipson et al.* [1994] observed similar behavior in the CIRRIS 1A 5.3 μm

Table 1. Summary of Conditions and Results for Auroral NO Data in Figure 3

Orbit	Scan	D/N/T	Latitude	SZA	Rotational Temperature, K	Spin-Orbit Ω = 1/2 Fraction	Spin-Orbit Temperature, K
8692	40	Day	−82.11	84.15	767	0.621	350
8692	41	Twilight	−76.81	89.35	733	0.620	353
8692	42	Twilight	−72.18	93.68	759	0.617	362
8692	43	Night	−67.47	97.99	757	0.614	372
8692	44	Night	−62.72	102.28	672	0.619	356
8692	45	Night	−57.81	107.20	617	0.618	359
8692	46	Night	−52.43	111.99	631	0.613	375
8697	41	Day	−72.87	61.82	720	0.612	379
8699	40	Day	−48.33	41.03	787	0.624	341
8699	41	Day	−53.98	45.12	803	0.616	365

Table 2. Summary of Conditions and Results for Quiescent NO Data in Figure 3

Scan	Day/ Night	Tangent Altitude, km	Latitude	SZA	Rotational Temperature, K	Spin-Orbit Ω = 1/2 Fraction	Spin-Orbit Temperature, K
4	Day	120.8	75.34	53.52	585	0.625	338
4	Day	131.0	75.34	53.52	642	0.630	324
4	Day	141.2	75.34	53.52	679	0.643	293
4	Day	151.3	75.34	53.52	752	0.662	257
4	Day	161.5	75.34	53.52	788	0.671	242
34	Night	122.7	−58.45	141.25	558	0.638	305
34	Night	132.9	−58.45	141.25	610	0.645	289
34	Night	143.2	−58.45	141.25	684	0.651	277
34	Night	153.5	−58.45	141.25	727	0.672	241
34	Night	163.7	−58.45	141.25	770	0.680	229

emission data taken during quiescent conditions. They determined that the subthermal NO(v = 1) spin-orbit distributions were most likely due to the formation of a NO_2 intermediate during the vibrational excitation of NO(v = 0) by impacts with O atoms. Previous studies of NO_2 photodissociation have measured subthermal spin-orbit populations in the NO(v = 0) and NO(v = 1) photofragments [*Hunter et al.*, 1993]. The NO produced by NO_2 photodissociation has a nascent Ω = 1/2 fraction of 0.7, corresponding to a spin temperature of 200 K. MIPAS and CIRRIS 1A data taken at the highest altitudes under quiescent conditions also have NO Ω = 1/2 fractions approaching 0.7 (see Table 2). Because the collision rate decreases with altitude, NO(v = 1) spin-orbit populations are most likely to resemble a nascent distribution at high altitudes. Spin-orbit relaxation of NO by collisions is slower by at least an order of magnitude compared to rotational relaxation [*Islam et al.*, 1995; *Funke and López-Puertas*, 2000]. At lower altitudes where collisions are important, the difference in the relaxation rates can result in NO(v = 1) emissions that are rotationally thermal but have non-LTE spin-orbit distributions.

3.3. Quiescent 5.3 μm NO Emission: Diurnal Variation

[18] The two most interesting results from Figure 3 are that the auroral NO has a hotter spin-orbit distribution (smaller Ω = 1/2 fraction) than the quiescent NO and that there is also a difference between the daytime and nighttime quiescent spin-orbit distributions. In order to explain the difference between the quiescent day and night spectra, it is important to consider the diurnal variability of the atmosphere and the various NO(v = 1) production mechanisms. The rate of collisional spin-orbit relaxation of NO may increase at higher kinetic temperatures. However, above an altitude of ~130 km, the radiative rate of NO(v = 1) is faster than the collisional rate. Therefore the observed day-night variation in NO spin-orbit ratio cannot be explained simply by diurnal variations in atmospheric temperature. Excitation of NO by O atom collisions and the $N(^4S) + O_2$ reaction are both sources of NO(v = 1) during the day and night [*Sharma et al.*, 1996b; *Sharma et al.*, 1998]. Solar pumping of NO(v = 0) and the $N(^2D) + O_2$ reaction are only important during the day. Solar pumping should not have an effect on the NO(v = 1) spin-orbit distribution. Thus the $N(^2D) + O_2$ reaction is identified as a possible cause of the quiescent day-night variation in the spin-orbit distributions, displayed in Figure 3 and summarized in Table 2. There is no reason to expect that NO produced by the $N + O_2$ reaction has the same spin-orbit distribution as NO produced by O atom collisional excitation. Although both of these processes may proceed through an NO_2 intermediate, the potential energy surfaces and the dynamics may be very different.

[19] Atmospheric modeling calculations have been conducted using the non-LTE model developed by *Funke and López-Puertas* [2000] in order to investigate the effect of varying the nascent NO spin-orbit distribution produced by the $N + O_2$ reaction under quiescent daytime and nighttime conditions. All parameters in the model are the same as described in the reference, except that the updated rate constant for process (1) measured by *Hwang et al.* [2003] was used, and the pressure, temperature, and N atom concentrations were taken from MSIS predictions for the date and geolocations of the MIPAS measurements. On the basis of the current results and the CIRRIS 1A measurements [*Lipson et al.*, 1994], the model assumes that O atom collisional excitation produces NO(v = 1) with a nascent spin-orbit temperature of 200 K, which corresponds to an Ω = 1/2 fraction of 0.7. There are no experimental measurements of the nascent NO spin-orbit distribution from the $N + O_2$ reaction, so the nascent spin-orbit temperature was varied between 200 K and 5000 K in the model. These values were chosen because 200 K is the nascent spin temperature of NO(v = 1) produced by collisional excitation of NO(v = 0) by O atoms and 5000 K is the nascent rotational temperature of NO produced by the $N + O_2$ reaction.

[20] The non-LTE modeling results for the NO(v = 1) spin-orbit ratio as a function of altitude are presented in Figure 4 for a nascent NO spin-orbit temperature from the $N + O_2$ reaction of (Figure 4a) 200 K and (Figure 4b) 5000 K for daytime (triangle symbols) and nighttime (square symbols). In Figure 4a, the day-night differences are only significant for altitudes below 130 km. At low altitudes, the rate of collisional spin-orbit relaxation is competitive with the rate of NO(v = 1) radiative emission. Thus the colder nighttime translational temperatures below 130 km result in slower collisional spin-orbit relaxation according to the model. Above 130 km, the translational temperature of the atmosphere does not have a significant effect on the model NO(v = 1) spin-orbit ratios. In Figure 4a, the model was run assuming that O atom collisional excitation and the $N + O_2$ reaction produce NO with the same nascent spin-orbit temperature. Thus little day-night

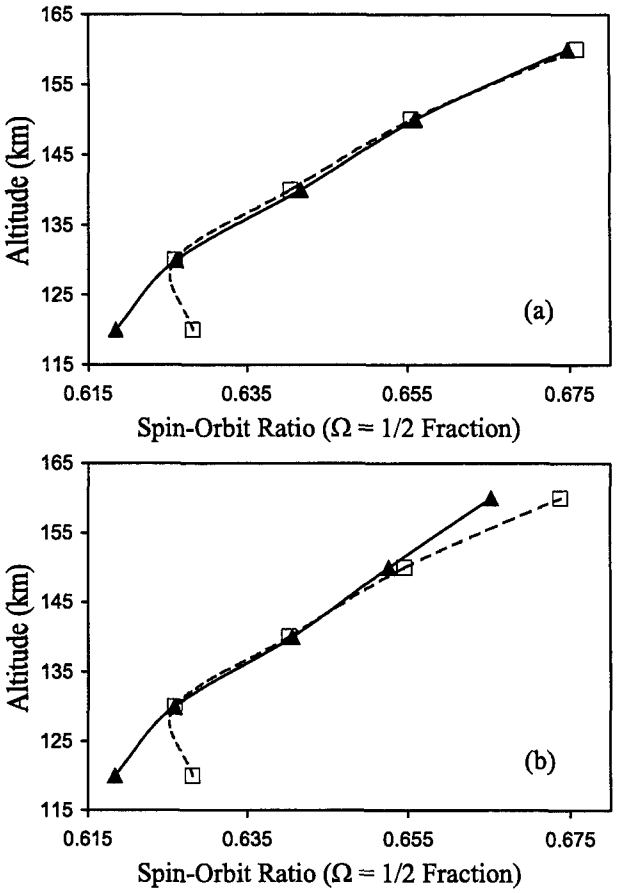

Figure 4. Non-LTE atmospheric model of NO(v = 1) spin-orbit ratios as a function of altitude for quiescent daytime (triangles) and nighttime (squares, dashed line) conditions. The model nascent NO spin-orbit temperature from the N + O_2 reaction was set to (a) 200 K and (b) 5000 K.

variation is expected at higher altitudes. In Figure 4b, the nascent NO spin temperature from N + O_2 was increased to 5000 K resulting in significant day-night variation above 150 km. The modeling results confirm that the nascent NO spin-orbit distribution produced by the N + O_2 reaction can influence the diurnal variability of the NO(v = 1) spin-orbit ratios in the upper atmosphere, similar to the effect observed in the MIPAS data. In Figure 4b, day-night variations are present below 130 km and above 150 km. In the MIPAS data presented in Figure 3, the day-night variation occurs over the whole range of tangent altitudes. The differences between the data and the model may largely be due to the fact that the values derived from the MIPAS spectra are representative of the LOS at the measured tangent altitude.

3.4. Auroral 5.3 μm NO Emission

[21] Our analysis has shown that NO(v = 1) data collected by MIPAS during the geomagnetic storm on 29 October has a hotter spin-orbit distribution than data taken under quiescent conditions. All of the auroral data in Figure 3 (diamond symbols) were taken at a tangent altitude of 68 km. As shown in Table 1, the auroral NO has rotational temperatures ranging from ~600 to 800 K. In comparison, NO observed on 14 June at the same tangent altitude under quiescent conditions has rotational temperatures of ~500–550 K. These temperatures are significantly higher than the kinetic temperature of the mesosphere (~220 K) at 68 km [*Mertens et al.*, 2004], further demonstrating that the majority of the MIPAS NO(v = 1) signal is coming from the thermosphere. Owing to the auroral activity, the rotational temperatures of the NO spectra recorded on 29 October were highly variable even for data taken only a couple of minutes apart and at similar latitudes (see Table 1). It is interesting to note that strong 5.3 μm emission signal levels did not always correlate with the highest rotational temperatures. Increased rotational temperatures and hotter spin-orbit distributions were observed by MIPAS for latitudes as low as 30°, consistent with visual observations of aurora at low latitudes during the October/November solar storm. Unfortunately, detailed information about the extent of the energy deposition along the LOS on 29 October is not readily available for correlation with the MIPAS data.

[22] Auroral activity has many effects on the atmosphere and on the production of NO, including significant atmospheric heating. The stronger the aurora, the greater the energy deposition rates and the more energy that is deposited at lower altitudes [*Thayer and Semeter*, 2004]. During an aurora, enhanced levels of energetic charged particles create increased amounts of N(^{4}S) and N(^{2}D) atoms, leading to greater chemical production of vibrationally excited NO. Thus the same reasoning that was used to explain the day-night variation in the quiescent data spin-orbit populations can also explain why the auroral NO has a different spin-orbit distribution. If the chemical reaction of N atoms with O_2 produces NO with a different spin-orbit distribution than O atom collisional excitation, then auroral activity should have a significant effect on the NO spin-orbit populations. Enhanced chemical production of NO(v = 1) during the aurora could explain why the spin-orbit Ω = 1/2 fractions are shifted even further to the left of the daytime quiescent data in Figure 3. The lack of diurnal variation in the auroral NO spin-orbit distributions is consistent with the fact that auroral activity can produce enhanced N atom concentrations during both the day and night. In the *Lipson et al.* [1994] study of NO spin-orbit distributions from the CIRRIS 1A experiment, one scan was recorded during nighttime auroral conditions at a tangent altitude of 205 km. In agreement with our results, the auroral NO had an increased rotational temperature and a spin-orbit Ω = 1/2 fraction that was shifted to the left compared with the quiescent data.

[23] The spin-orbit ratios for the auroral NO data are very similar for a range of different rotational temperatures (see Table 1). As a result, the auroral data points lie almost on a vertical line in Figure 3. This behavior confirms that NO spin-orbit relaxation occurs on a slower time scale than rotational relaxation. In fact, *Funke and López-Puertas* [2000] have determined that NO collisions with O atoms that result in internal relaxation have at least a 90% propensity to conserve the NO spin-orbit state. There have been no experimental measurements of NO spin-orbit relaxation by O atoms, but *Islam et al.* [1995] did observe a strong propensity for spin-orbit conservation in NO collisions with Ar and He. Although the auroral data in Figure 3 lie on a vertical line, it is not possible to derive

auroral NO spin-orbit distributions as a function of altitude from MIPAS data taken at only one tangent altitude. The MIPAS results indicate that auroral NO has a hotter spin-orbit distribution than quiescent data. The NO spin-orbit ratio is a longer lived signature of chemical reactivity than the rotational temperature because of the slower rate of spin-orbit relaxation. Therefore it should be possible to use the NO spin-orbit ratio to monitor auroral activity and to distinguish between NO(v = 1) produced by chemical reaction and NO(v = 1) created by O atom collisional excitation.

[24] This study demonstrates the need for additional measurements of NO spin-orbit distributions as a function of altitude under auroral conditions. The ability to synchronize MIPAS upper atmosphere measurements with auroral activity is limited because the major scientific objective of the instrument is focused on the stratosphere, and programming the instrument observation mode for the upper atmosphere requires a week of preparation time. However, very recently, new measurements have been made by the MIPAS instrument in the special upper atmosphere mode following a solar proton event in January 2005. These measurements will help to improve our understanding of non-LTE rotational and spin-orbit distributions under auroral conditions. In addition, future laboratory measurements of the nascent NO spin-orbit populations produced by the reactions of N(^{4}S) and N(^{2}D) atoms with O_2 would also be helpful for modeling non-LTE spin-orbit effects in the atmosphere.

4. Conclusions

[25] The 5.3 μm emissions recorded by the MIPAS instrument during the solar storm of October/November 2003 have been compared with data taken during quiescent conditions in order to investigate the effect of auroral activity on the NO state distributions. The NO(v = 1) spin-orbit distributions were found to be subthermal for all measurements. Under quiescent conditions, the NO(v = 1) spectra collected during the daytime had decreased spin-orbit Ω = 1/2 fractions compared with the nighttime measurements. The N(^{2}D) + O_2 reaction, which only produces significant amounts of NO(v) during the daytime, was identified as a possible source of the day-night differences. During the aurora, the NO(v = 1) spectra displayed enhanced rotational temperatures and decreased spin-orbit Ω = 1/2 fractions compared with the quiescent data. The auroral and quiescent measurements both indicate that vibrationally excited NO produced by chemical reaction has a hotter spin-orbit distribution than NO produced by O atom collisional excitation. Therefore the spin-orbit ratio may be used to distinguish between NO formed by different mechanisms. The ability to identify and quantify the sources of NO(v) in the upper atmosphere is important for determining the atmospheric energy budget. Future work will focus on the analysis of new MIPAS upper atmosphere mode data and on a more extensive comparison of the quiescent NO MIPAS data with the non-LTE atmospheric model. The modeling study will include a thorough investigation of the parameters that control the model NO(v = 1) spin-orbit ratio such as the spin-orbit relaxation rate and the separate contributions of the N(^{4}S) and N(^{2}D) + O_2 reactions.

[26] **Acknowledgments.** The authors acknowledge ESA for providing MIPAS spectra. J. L. Gardner, S. M. Miller, and S. J. Lipson were supported by the Air Force Office of Scientific Research under task 2303ES/92VS04COR. R. D. Sharma received partial support from the Geospace Sciences program, Office of Space Science, NASA under research grant SRT03-0015. The IAA team was partially supported by Spanish projects REN2001-3249/CLI and ESP2004-01556. B. Funke has been supported through a European Community Marie Curie Fellowship.

[27] Arthur Richmond thanks Jack A. Kaye and Martin Mlynczak for their assistance in evaluating this paper.

References

Amiot, C. (1982), The infrared emission spectrum of NO: Analysis of the Δv = 3 sequence up to v = 22, *J. Mol. Spectrosc.*, *94*, 150.

Armstrong, P. S., S. J. Lipson, J. A. Dodd, J. R. Lowell, W. A. M. Blumberg, and R. M. Nadile (1994), Highly rotationally excited NO (v, J) in thermosphere from CIRRIS 1A limb radiance measurements, *Geophys. Res. Lett.*, *21*, 2425.

Ballard, J., B. J. Kerridge, P. E. Morris, and F. W. Taylor (1993), Observations of v = 1 − 0 emission from thermospheric nitric oxide by ISAMS, *Geophys. Res. Lett.*, *20*, 1311.

Clancy, R. T., D. W. Rusch, and D. O. Muhleman (1992), A microwave measurement of high levels of thermospheric nitric oxide, *Geophys. Res. Lett.*, *19*, 261.

Dothe, H., J. W. Duff, R. D. Sharma, and N. B. Wheeler (2002), A model of odd nitrogen in the aurorally dosed nighttime terrestrial thermosphere, *J. Geophys. Res.*, *107*(A6), 1071, doi:10.1029/2001JA000143.

Duff, J. W., and R. D. Sharma (1997), Quasiclassical trajectory study of NO vibrational relaxation by collisions with atomic oxygen, *J. Chem. Soc. Faraday Trans.*, *93*, 2645.

Duff, J. W., F. Bien, and D. E. Paulsen (1994), Classical dynamics of the N(^{4}S) + O_2($X^3\Sigma_g^-$) → NO($X^2\Pi$) + O(^{3}P) reaction, *Geophys. Res. Lett.*, *21*, 2043.

Duff, J. W., H. Dothe, and R. D. Sharma (2003), On the rate coefficient of the N(^{2}D) + O_2 → NO + O reaction in the terrestrial thermosphere, *Geophys. Res. Lett.*, *30*(5), 1259, doi:10.1029/2002GL016720.

Duff, J. W., H. Dothe, and R. D. Sharma (2005), A first-principles model of spectrally resolved 5.3 μm nitric oxide emission from aurorally dosed nighttime high-altitude terrestrial thermosphere, *Geophys. Res. Lett.*, doi:10.1029/2005GL023124, in press.

European Space Agency (2000), ENVISAT-MIPAS: An instrument for atmospheric chemistry and climate research, *ESA SP-1229*, 124 pp., Noordwijk, Netherlands.

Funke, B., and M. López-Puertas (2000), Nonlocal thermodynamic equilibrium vibrational, rotational, and spin state distribution of NO(v = 0, 1, 2) under quiescent atmospheric conditions, *J. Geophys. Res.*, *105*, 4409.

Funke, B., M. López-Puertas, G. Stiller, T. von Clarmann, M. Höpfner, and M. Kuntz (2000), Non-LTE state distribution of nitric oxide and its impact on the retrieval of the stratospheric daytime NO profile from MIPAS limb sounding instruments, *Adv. Space Res.*, *26*, 947.

Funke, B., M. López-Puertas, G. Stiller, T. von Clarmann, and M. Höpfner (2001), A new non-LTE retrieval method for atmospheric parameters from MIPAS-ENVISAT emission spectra, *Adv. Space Res.*, *27*, 1099.

Hunter, M., S. A. Reid, D. C. Robie, and H. Reisler (1993), The monoenergetic unimolecular reaction of expansion-cooled NO_2: NO product state distributions at excess energies 0–3000 cm^{-1}, *J. Chem. Phys.*, *99*, 1093.

Hwang, E. S., K. J. Castle, and J. A. Dodd (2003), Vibrational relaxation of NO(v = 1) by oxygen atoms between 295 and 825 K, *J. Geophys. Res.*, *108*(A3), 1109, doi:10.1029/2002JA009688.

Islam, M., I. W. M. Smith, and J. W. Wiebrecht (1995), Rate coefficients for state-to-state rovibronic relaxation in collisions between NO($X^2\Pi$, v = 2, Ω, J) and NO, He, and Ar at 295, 200, and 80 K, *J. Chem. Phys.*, *103*, 9676.

Kaye, J. A., and J. B. Kumer (1987), Nonlocal thermodynamic equilibrium effects in stratospheric NO and implications for infrared remote sensing, *Appl. Opt.*, *26*, 4747.

Kovacs, I. (1969), *Rotational Structure in the Spectra of Diatomic Molecules*, 320 pp., Elsevier, New York.

Lipson, S. J., P. S. Armstrong, J. A. Dodd, J. R. Lowell, W. A. M. Blumberg, and R. M. Nadile (1994), Subthermal nitric oxide spin-orbit distributions in the thermosphere, *Geophys. Res. Lett.*, *21*, 2421.

Mertens, C. J., et al. (2004), SABER observations of mesospheric temperatures and comparisons with falling sphere measurements taken during the 2002 summer MaCWAVE campaign, *Geophys. Res. Lett.*, *31*, L03105, doi:10.1029/2003GL018605.

Miller, S. M., R. D. Sharma, J. W. Duff, and H. Dothe (2003), Vibration-rotation distribution of the nascent NO produced by the N(^{2}D) + O_2 reaction, *Geophys. Res. Abstracts*, *5*, EAE 03-A-4630.

Mlynczak, M., et al. (2003), The natural thermostat of nitric oxide emission at 5.3 μm in the thermosphere observed during the solar storms of April 2002, *Geophys. Res. Lett.*, *30*(21), 2100, doi:10.1029/2003GL017693.

Murphy, R. E., E. T. P. Lee, and A. M. Hart (1975), Quenching of vibrationally excited nitric oxide by molecular oxygen and nitrogen, *J. Chem. Phys.*, *63*, 2919.

Rawlins, W. T., J. C. Person, M. E. Fraser, S. M. Miller, and W. A. M. Blumberg (1998), The dipole moment and infrared transition strengths of nitric oxide, *J. Chem. Phys.*, *109*, 3409.

Rusch, D. W., J.-C. Gérard, and C. G. Fesen (1991), The diurnal variation of NO, $N(^2D)$, and ions in the thermosphere: A comparison of satellite measurements to a model, *J. Geophys. Res.*, *96*, 11,331.

Sætre, C., J. Stadsnes, H. Nesse, A. Aksnes, S. M. Petrinec, C. A. Barth, D. N. Baker, R. R. Vondrak, and N. Østgaard (2004), Energetic electron precipitation and the NO abundance in the upper atmosphere: A direct comparison during a geomagnetic storm, *J. Geophys. Res.*, *109*, A09302, doi:10.1029/2004JA010485.

Sharma, R. D., and J. W. Duff (1997), Determination of the translational temperature of the high altitude terrestrial thermosphere from the rotational distribution of the 5.3 μm emission from NO($v = 1$), *Geophys. Res. Lett.*, *24*, 2407.

Sharma, R. D., Y. Sun, and A. Dalgarno (1993), Highly rotationally excited nitric oxide in the terrestrial thermosphere, *Geophys. Res. Lett.*, *20*, 2043.

Sharma, R. D., H. Dothe, and F. von Esse (1996a), On the rotational distribution of the 5.3 μm "thermal" emission from nitric oxide in the nighttime terrestrial thermosphere, *J. Geophys. Res.*, *101*, 17,129.

Sharma, R. D., H. Dothe, F. von Esse, V. A. Kharchenko, Y. Sun, and A. Dalgarno (1996b), Production of vibrationally and rotationally excited NO in the nighttime terrestrial thermosphere, *J. Geophys. Res.*, *101*, 19,707.

Sharma, R. D., H. Dothe, and J. W. Duff (1998), Model of the 5.3 μm radiance from NO during the sunlit terrestrial thermosphere, *J. Geophys. Res.*, *103*, 14,753.

Sharma, R. D., R. O'Neil, H. Gardiner, J. Gibson, H. Dothe, J. W. Duff, P. P. Wintersteiner, and M. Kendra (2001), Midcourse Space Experiment: Auroral enhancement of nitric oxide medium-wave infrared emission observed by the Spatial Infrared Imaging Telescope III radiometer, *J. Geophys. Res.*, *106*, 21,351.

Simpson, S. (2003), Massive solar storms inflict little damage on Earth, *Space Weather*, *1*(2), 1012, doi:10.1029/2003SW000042.

Siskind, D. E., C. A. Barth, and J. M. Russell III (1998), A climatology of nitric oxide in the mesosphere and thermosphere, *Adv. Space Res.*, *21*, 1353.

Skoug, R. M., J. T. Gosling, J. T. Steinberg, D. J. McComas, C. W. Smith, N. F. Ness, Q. Hu, and L. F. Burlaga (2004), Extremely high speed solar wind: 29–30 October 2003, *J. Geophys. Res.*, *109*, A09102, doi:10.1029/2004JA010494.

Solomon, S. C., C. A. Barth, and S. M. Bailey (1999), Auroral production of nitric oxide measured by the SNOE satellite, *Geophys. Res. Lett.*, *26*, 1259.

Thayer, J. P., and J. Semeter (2004), The convergence of magnetospheric energy flux in the polar atmosphere, *J. Atmos. Sol. Terr. Phys.*, *66*, 807.

Vitt, F. M., T. E. Cravens, and C. H. Jackman (2000), A two-dimensional model of thermospheric nitric oxide sources and their contributions to the middle atmospheric chemical balance, *J. Atmos. Sol. Terr. Phys.*, *62*, 653.

B. Funke and M. Lopéz-Puertas, Instituto de Astrofísica de Analucía (CSIC), Apartado Postal 3004, E-18080 Granada, Spain.

J. L. Gardner, Stewart Radiance Laboratory, 139 The Great Road, Bedford, MA 01730, USA. (jennifer.gardner@hanscom.af.mil)

S. J. Lipson, S. M. Miller, and R. D. Sharma, Space Vehicles Directorate, Air Force Research Laboratory, 29 Randolph Road, Hanscom Air Force Base, MA 01731, USA.